Using Normal Component Magnetograms in 3D Data-Driven Simulations: A Comparison of Two Electric Field Inversion Techniques

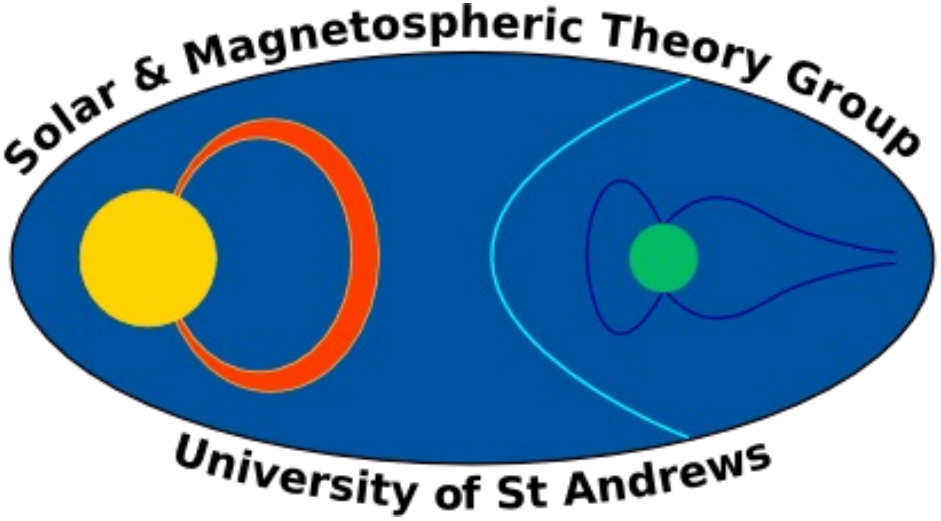

Duncan H. Mackay

University of St Andrews

Published Paper: Mackay and Yeates (2021), Solar Physics, 296

Structure

- Data-Driven Models: Input Data and Restrictions.
- Comparison of new “Sparse” and “Non-Sparse” Techniques.
- Overview of Gibb, Mackay and Green (2014)
  - formation and eruption of X-ray Sigmoid.
  - data-driven using old ‘Non-Sparse’ technique.
- Comparison of Sparse and Non-Sparse Techniques – Gibb et al. (2014) – which is best ?
- Overview and Future Studies.

Overview

- Overall goal: understand how magnetic energy and helicity is injected into the corona through motions in the solar photosphere.

  reproduce and then predict solar phenomena

- Lower Boundary: **v** – plasma velocity, **B** – magnetic field → **E = - v x B**

  Data Constrained — analytical, obs. const.

  Data Driven — obs. input

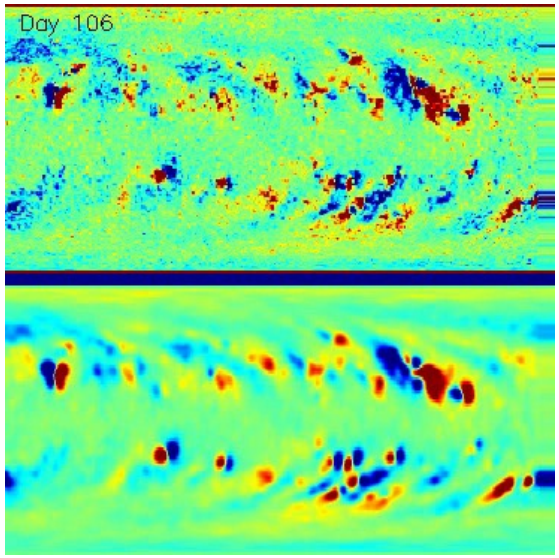

Global Sun

(A Yeates)

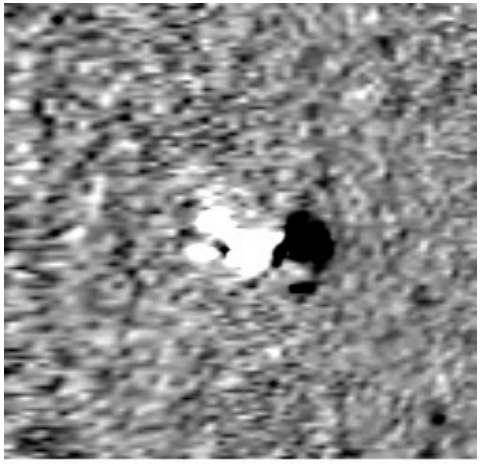

Active Region

Mackay, Green and van Ballegooijen (2011), Cheung and DeRosa (2012), Gibb et al. (2020) Yang et al., (2012), Kazachenko, Fisher, and Welsch (2014), Hayashi et al. (2018), Pomoell, Lumme, and Kilpua (2019); Hoeksema et al. (2020)

- Requirements for full data driven simulations:

  Vector magnetograms – only known in strong field regions > 250G.

  Velocity Field – doppler and local correlation tracking.

  SDO – significant amount of data processing (Kazachenko et al. (2015), Hoeksema et al.2020)

- Approximate technique: normal component magnetograms.

  Pro: strong/weak field regions and fast.

  Con: approximate electric field (Pomoell et al. 2019)

- Why $\mathbf{E}_h = -\nabla \times (\Phi \hat{\mathbf{z}}) - \nabla_h \Psi$

  Inductive — Non-Inductive

$$\frac{\partial B_z}{\partial t} = -\hat{\mathbf{z}}.(\nabla \times \mathbf{E}_h)$$

$$\frac{\partial B_z}{\partial t} = -\nabla^2 \Phi.$$

- Cannot constrain non-inductive term

$$\Psi = 0$$

(Mikic et al. 1999, Amari et al. 2003, Mackay et al. 2011)

- Electric field – non-localized

$$\mathbf{B} \neq \mathbf{0} \text{ and } \mathbf{v} \neq \mathbf{0}$$

Breaks Ohm's law

- Why develop techniques based on normal component magnetograms ?

  (i) Allows data-driven techniques to be applied to pre- SDO data.

  (ii) If SDO or identical observations are no longer available, driven simulations may still be run (L5 – normal component magnetograph).

  (iii) It allows data-driven simulations to be carried out in Quiet Sun locations.

- Mackay et al. (2011) – data-driven technique
  - used by Gibb/Yardley/Pagano – S^2WARM

- Yeates (2017) – new method for computing E_h from B_z - 2D simulations.
  - include non-inductive component.
  - minimise number of locations E_h non-zero (sparse).
  - more realistic representation of physical system ???

- Compare Yeates (2017) and Mackay et al. (2011) techniques – 3D simulations

The Model(s)

- Corona:

$$\mathbf{B} = \nabla \times \mathbf{A}$$

$$\frac{\partial \mathbf{A}}{\partial t} = -\mathbf{E} \qquad \mathbf{E} = -\mathbf{v} \times \mathbf{B} + \eta \mathbf{j} \qquad \mathbf{v} = \frac{\mathbf{j} \times \mathbf{B}}{\nu B^2}$$

Coronal field evolves through a series of quasi-static force-free states **(j x B = 0).**

Relaxation time scale ~ not physical.

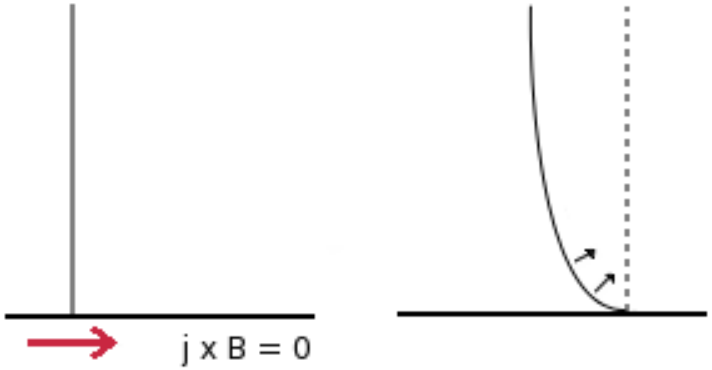

- Photosphere:

$$\mathbf{A}_h(x, y, 0, t) = (A_{xh}, A_{yh})$$

$$B_z(x, y, 0, t_k) = \left(\frac{\partial A_{yh}}{\partial x} - \frac{\partial A_{xh}}{\partial y} \right) \qquad \frac{\partial B_z}{\partial t} = -\hat{\mathbf{z}}.(\nabla \times \mathbf{E}_h)$$

$$\mathbf{E}_h(x, y, 0, t) = (E_{xh}, E_{yh})$$

- Mackay et al. (2011) – Non-Sparse

$$\mathbf{E}_h = -\nabla \times (\Phi \hat{\mathbf{z}}) - \nabla_h \Psi$$

$$\frac{\partial B_z}{\partial t} = -\hat{\mathbf{z}}.(\nabla \times \mathbf{E}_h)$$

$$\frac{\partial B_z}{\partial t} = -\nabla^2 \Phi. \quad \Psi = 0$$

- Solved using multi-grid technique

- Equilivent to L_2 – norm.

$$|| x ||_2^2 = \sum_i x_i^2$$

- Yeates (2017) – Sparse

$$\int_s \frac{\partial B_z}{\partial t} ds = -\oint_l \mathbf{E}_h.\mathbf{dl}$$

$$\frac{\partial B_z^{i,j}}{\partial t} = \frac{\Delta x E_{xh}^{i,j+1/2} - \Delta x E_{xh}^{i,j-1/2} + \Delta y E_{yh}^{i-1/2,j} - \Delta y E_{yh}^{i+1/2,j}}{\Delta x \Delta y}$$

$$A\mathbf{x} = \mathbf{b}$$

$$\mathbf{x} = [E_{xh}, E_{uh}], \mathbf{b} = \partial B_z / \partial t$$

$$\text{A is a } n^2 \times 2n(n+1)$$

- Basis pursuit – minimise L_1 - norm

$$|| x ||_1 = \sum_i | x_i |$$

- Solving for $\mathbf{A_h}$ instead of $\mathbf{E_h}$ use B_z .

$$\mathbf{A_h} = \nabla \times (\phi(x,y)\hat{\mathbf{z}})$$

$$\nabla^2 \phi = -Bz.$$

$$\frac{\partial \mathbf{A}}{\partial t} = -\mathbf{E}$$

$$B_z^{i,j} = \frac{\Delta x A_{xh}^{i,j+1/2} - \Delta x A_{xh}^{i,j-1/2} + \Delta y A_{yh}^{i-1/2,j} - \Delta y A_{yh}^{i+1/2,j}}{\Delta x \Delta y}$$

Overview of Gibb, Mackay and Green (2014)

- Use magnetogram observations and 3D NLFF modelling to reproduce the formation/eruption of a sigmoid (Mackay et al 2011).

- Gibb et al. 2014: AR10977, 2nd -10th Dec 2007 (Green et al. 2011)

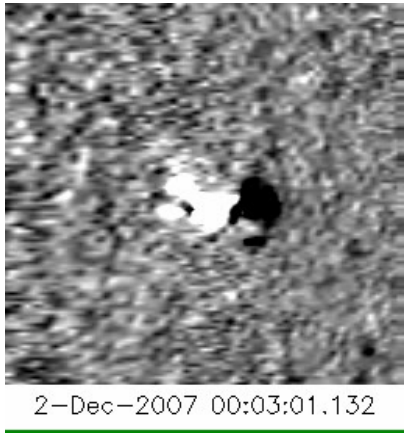

7th Dec 04:14UT

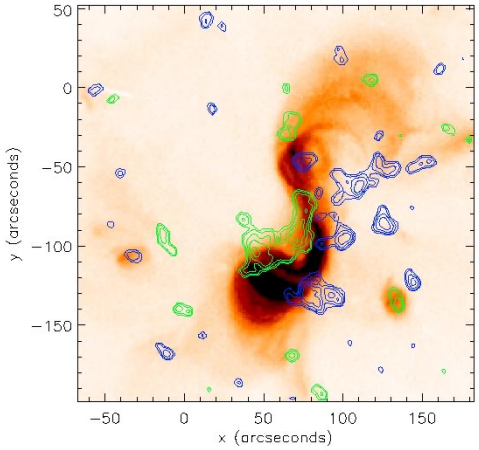

Main features:

Bipolar Form (cancellation, rotation).

Formation / Eruption of X-Ray Sigmoid.

B1.4 GOES Flare.

- Flux Variation

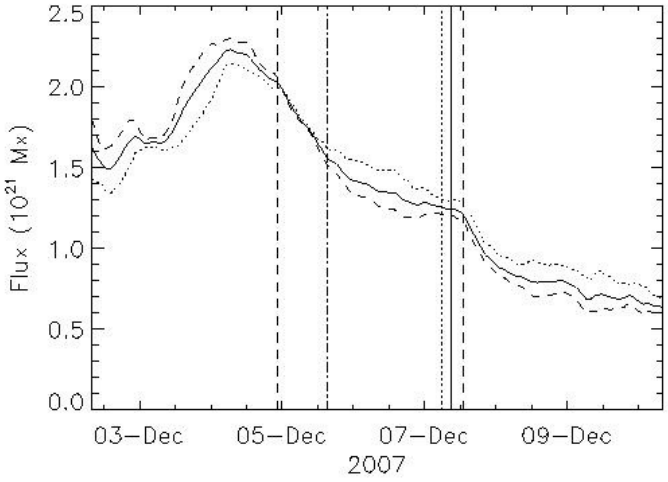

Flux Cancellation events (vertical dashed)

GOES B1.4 Flare (vertical dotted)

Rotation of AR

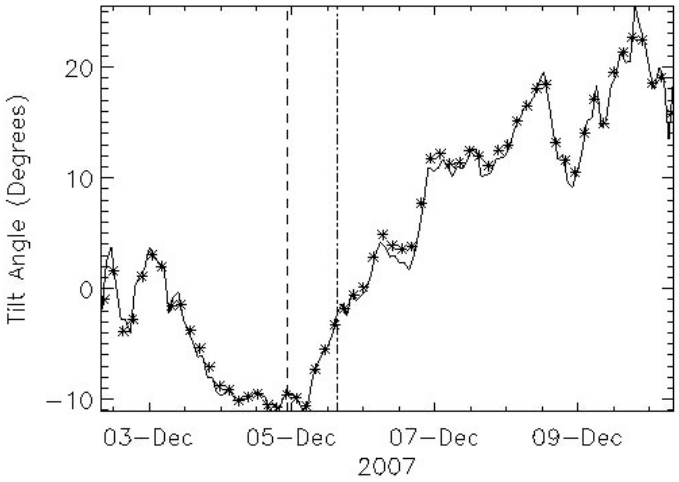

Non-sparse model

- Photosphere – direct input of 96 min MDI observations (Mackay et al. 2011)

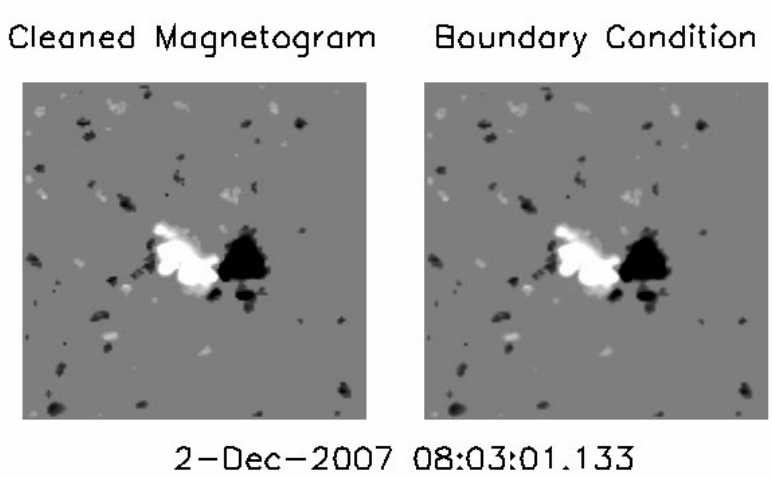

$$\Rightarrow \quad A_{xb}(x,y,k) = \frac{\partial \Phi}{\partial y} \qquad \frac{\partial^2 \Phi}{\partial x^2} + \frac{\partial^2 \Phi}{\partial y^2} = -B_z$$

$$A_{yb}(x,y,k) = -\frac{\partial \Phi}{\partial x}$$

$B_z(t) \rightarrow A_{xb}(t), A_{yb}(t)$; $B_z(t+1) \rightarrow A_{xb}(t+1), A_{yb}(t+1)$

- Technique produces an accurate representation of observed magnetograms.

- Consider evolution of coronal magnetic field – study injection and storage of energy.

Evolution of Field lines

Initial Condition:
Potential Field
08:03 UT 2nd Dec

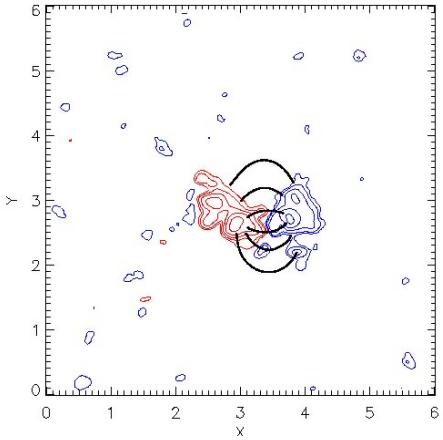

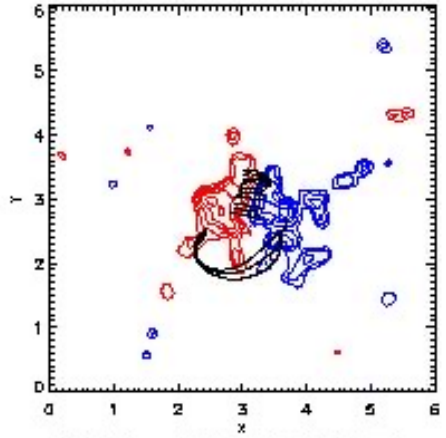

05–Dec–2007 00:00:01 UT

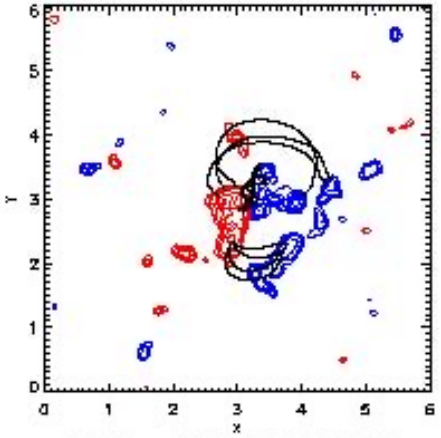

05–Dec–2007 20:47:01 UT

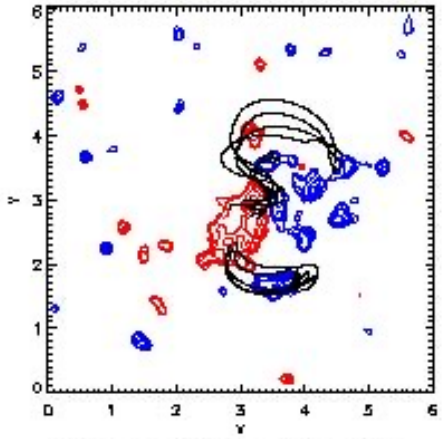

06–Dec–2007 17:36:01 UT

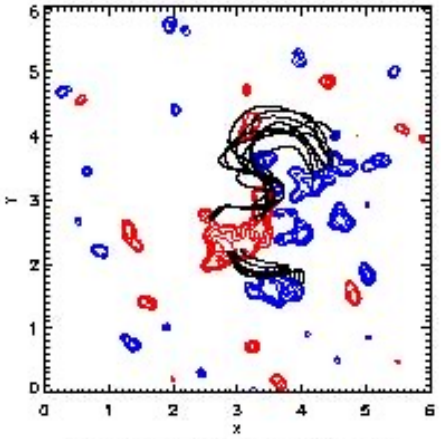

07–Dec–2007 04:48:01 UT

5th Dec 09:35 UT

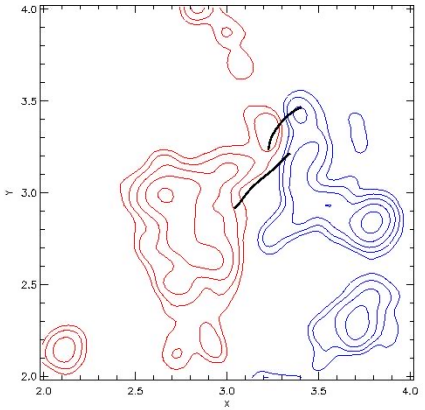

5th Dec 14:23 UT

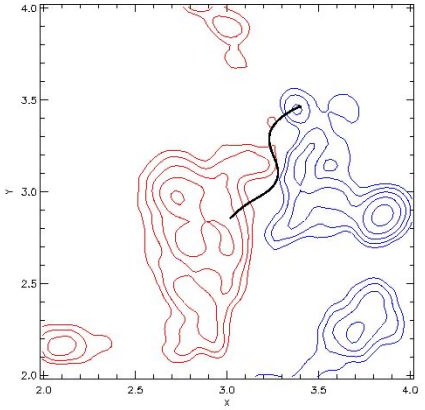

- Flux rope forms at the site of the sigmoid: flux cancellation.
- Flux rope flux peaks at 2.5×10^{20}Mx (20% of the active region flux)
- Do we match the observations?

Comparison with Observations

7th Dec 04:48 UT

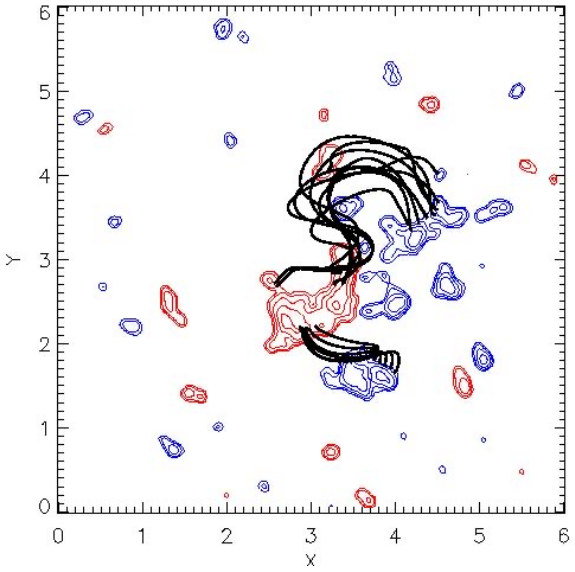

7th Dec 04:14 UT

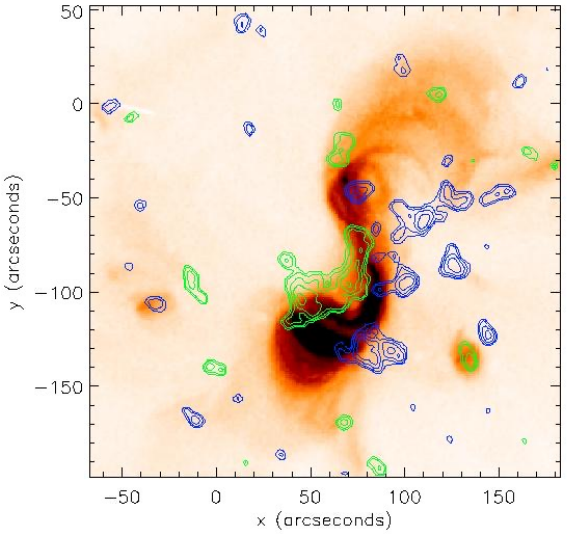

- Simulation reproduces key features of the observations.

- Varying initial condition:
  - LFFF +ve α
    - Improves fit at south
    - Worse at north
  - Optimal i.c. NLFFF
    - Northern part (α = 0)
    - Southern part (α > 0)

- GOES Flare 04:20 UT.

- Flux rope looses stability between 05.50 and 07:20 on 7th Dec (1-2 96min MDI frames)

- Follow build up of flux rope and stress to point of eruption: twist > 2pi

7th Dec 07.20 UT

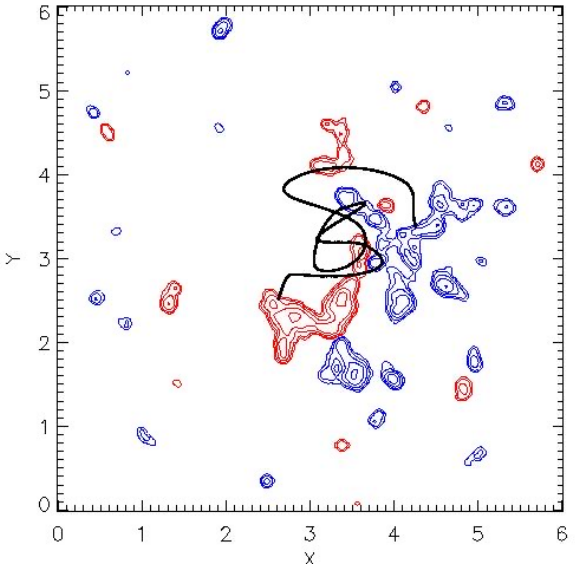

Magnetic Energy and Helicity

Free Magnetic Energy

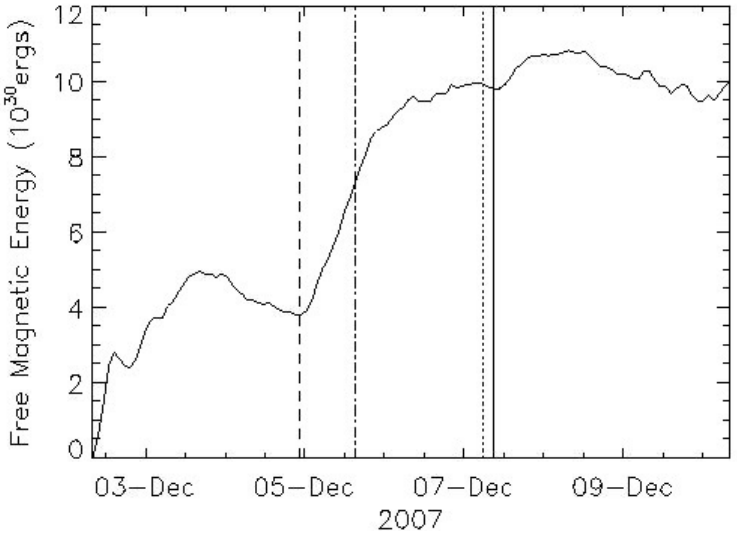

Relative Helicity

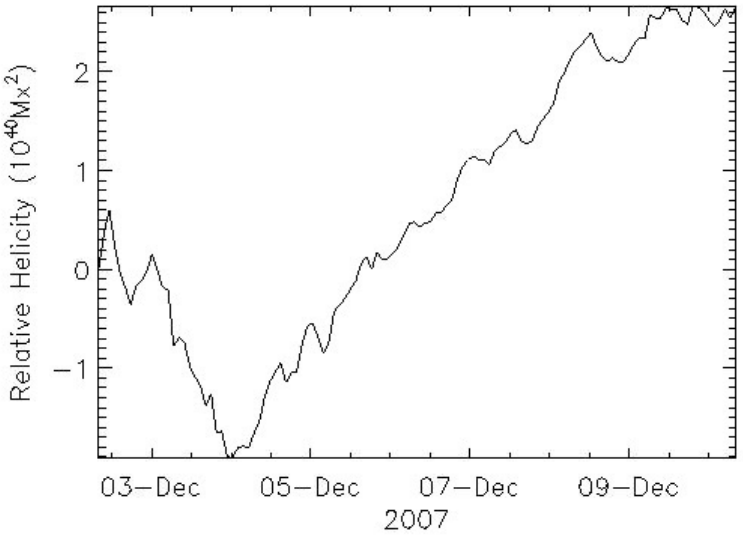

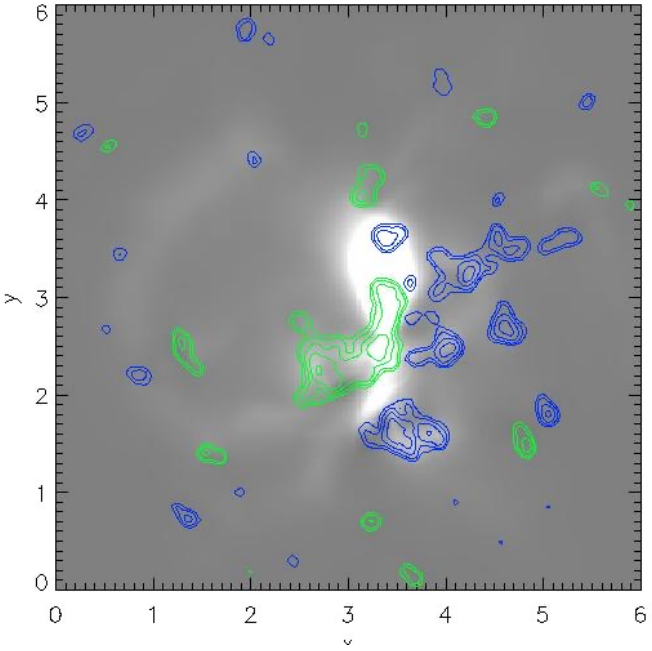

- Sharp rise in free energy at first cancellation: free energy stored in flux rope.
- Simulation breaks down (solid line) just after time of B1.4 flare (dotted): free energy 10^{31} ergs.
- Helicity follows variation of tilt angle.

Comparison of Sparse/Non-Sparse $\mathbf{E}_h$

- Compared 7 different simulations + potential field extrapolations:

  non-sparse, sparse, solving for **E** and **A**, ideal, non-ideal, varying start time.

Name	Duration (days)	Coronal Diffusion (km^2s^{-1})	Norm	Notes
run1	8	0	L_2	blue solid line Repeat of Gibb *et al.* (2014)
run1_ej	8	60	L_2	green solid line
run1_late	6	0	L_2	blue dashed Start on 4^{th} December 06:24
sparseA	8	0	L_1	black solid line
sparseA_ej	8	60	L_1	red solid line
sparseA_late	6	0	L_1	black dashed Start on 4^{th} December 06:24
sparseE	8	0	L_1	black dotted line
poten	8	0	N/A	yellow dash-dot line Potential Field extrapolation

- Potential field initial condition: 08:03 UT 2nd Dec or 06:24 UT 4th Dec.
- Ideal and non-ideal: $\eta = 0$ or 60 km^2s^{-1}
- Mackay et al. (2011) – non-sparse produces identical results when solving for E and A.

Comparison of Sparse and Non-Sparse E_h

- Driving Electric Field: 5th December 09:35

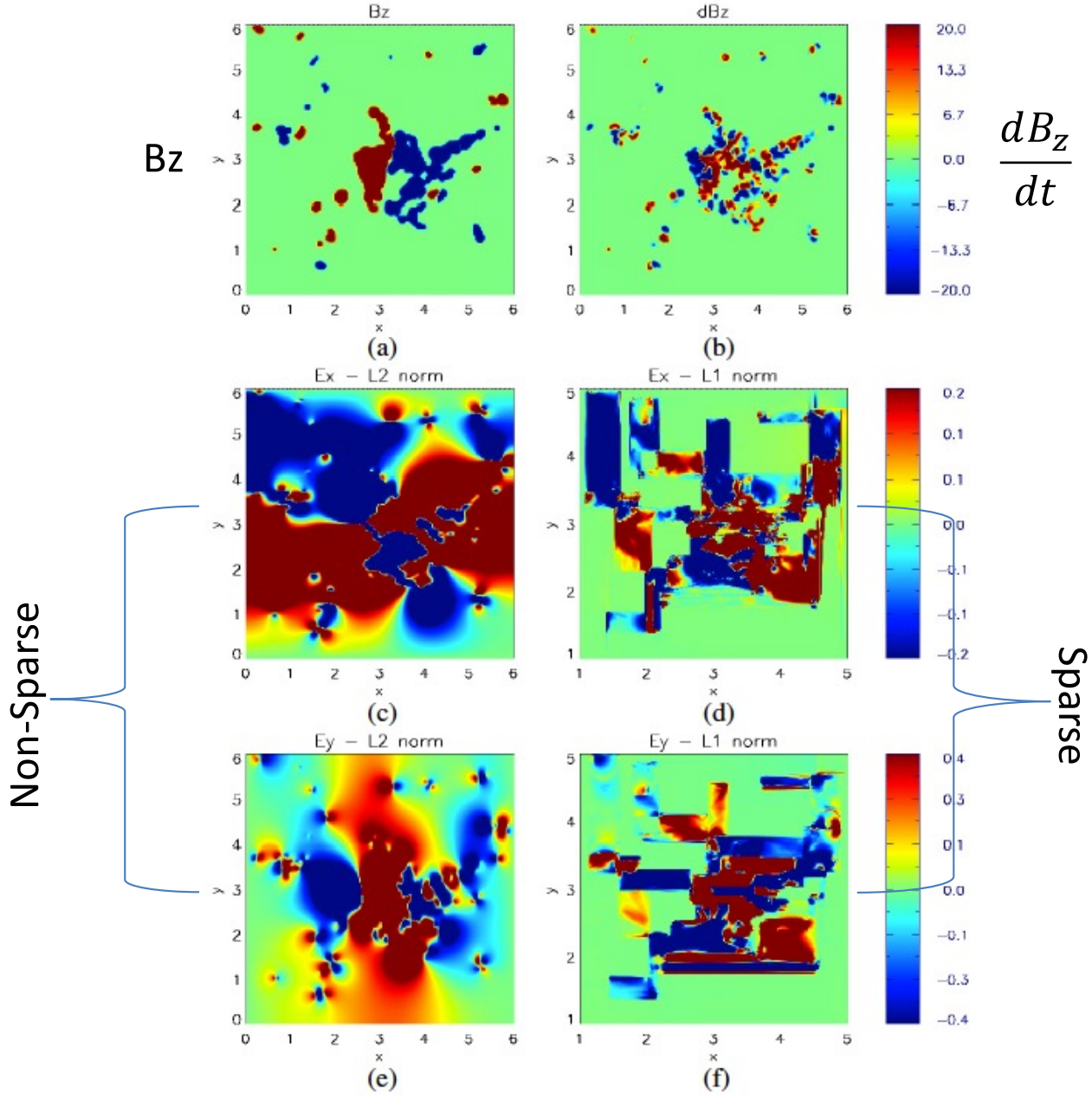

- Bipole: fragmented structure.
- Significant separation on own spatial scale.
- E_h saturate at low level: 1/100 peak.
- Both give same $\frac{dB_z}{dt}$
- Non-sparse:
  - smooth
  - non-zero everywhere.
- Sparse:
  - zero at many locations.
  - banded structure
  - localization depends on localization of B_z and $\frac{dB_z}{dt}$

Energy and Relative Helicity

- Total and Free magnetic Energy

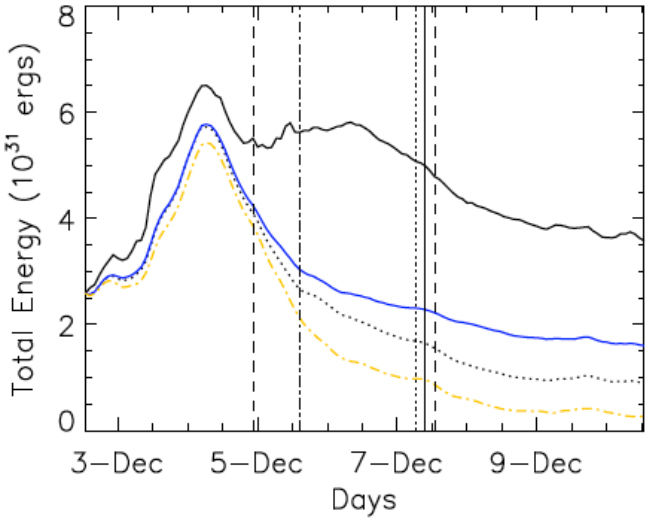

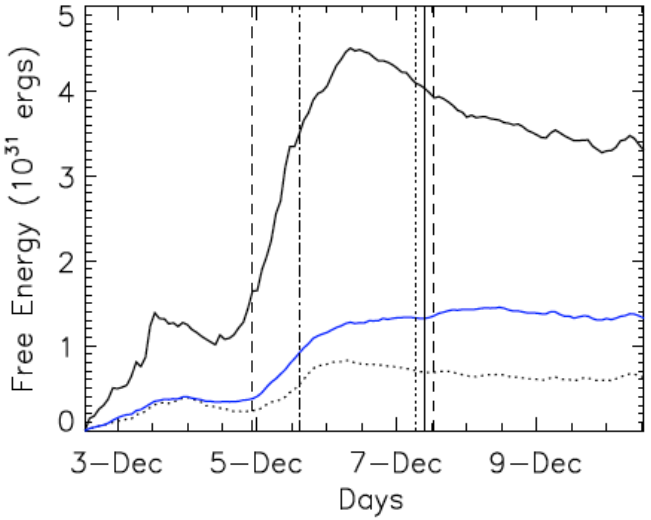

- Relative Helicity (Coulomb Gauge)

$$H_r = \int_V (\mathbf{A} + \mathbf{A_p}) \,.\, (\mathbf{B} - \mathbf{B_p})\, d\tau$$

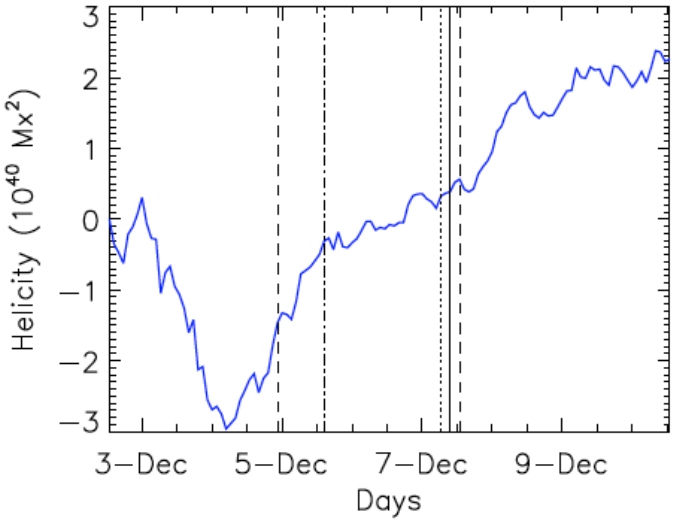

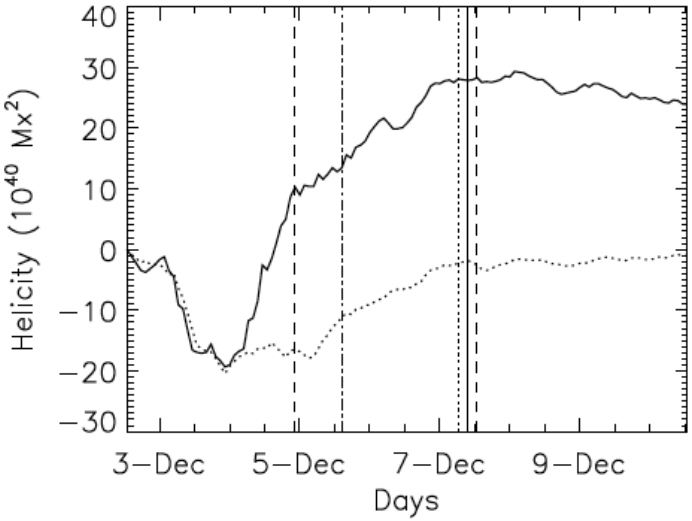

Black – sparse A

Black dashed - sparse E

Blue – non-sparse

Yellow – Potential Field

Field lines

5th Dec 00:00UT

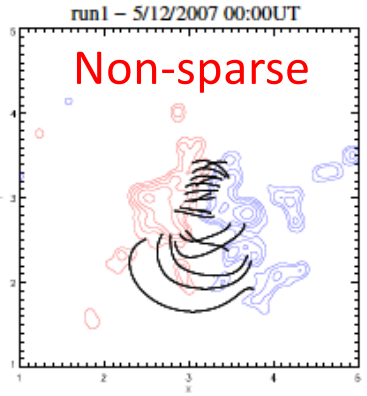

(a)

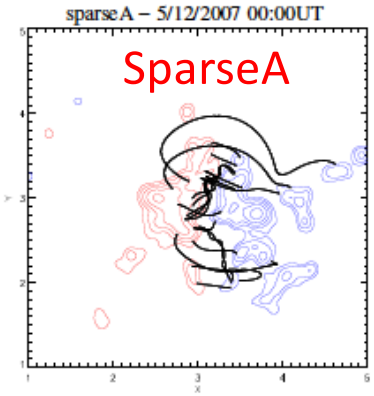

(b)

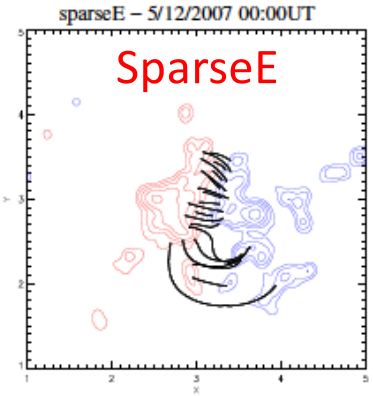

(c)

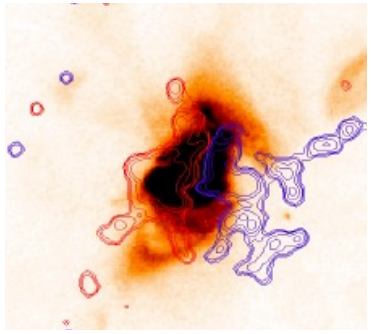

5th Dec 20:47UT

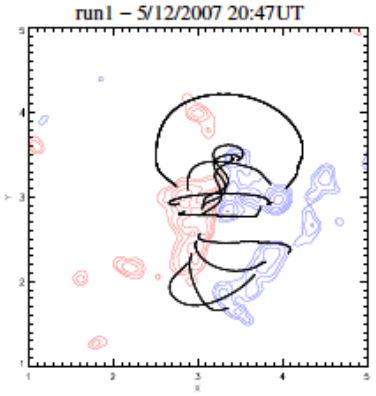

(d)

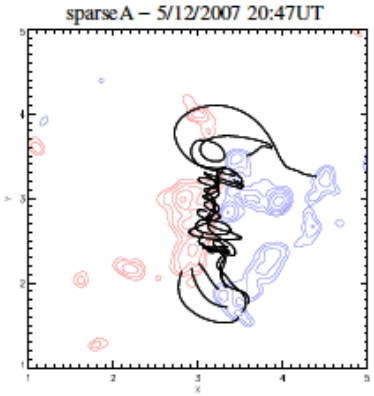

(e)

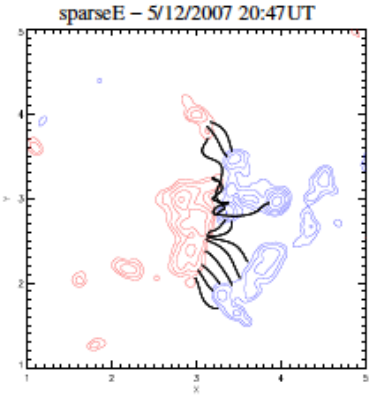

(f)

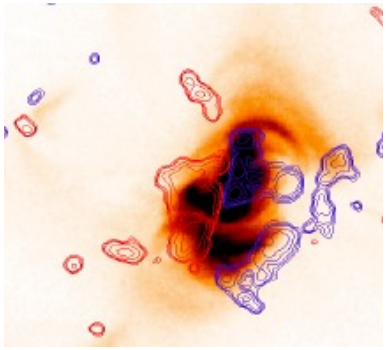

6th Dec 17:36UT

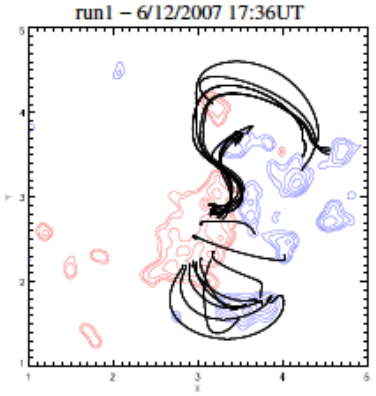

(g)

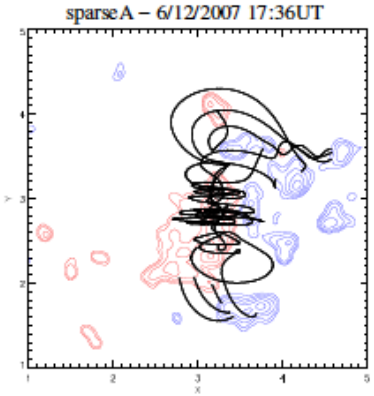

(h)

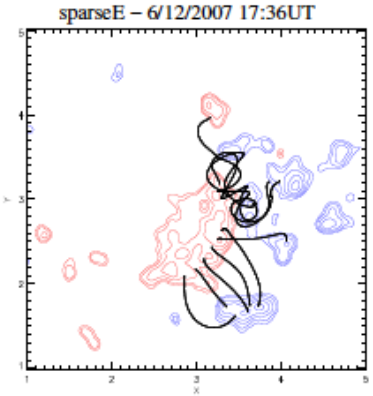

(i)

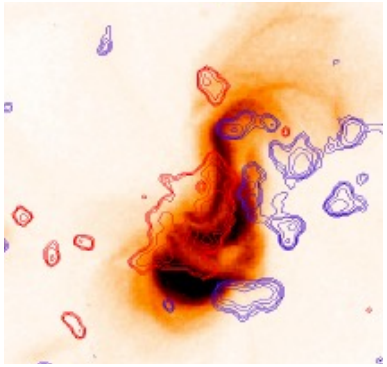

Sigmoid Field Lines –Oblique View

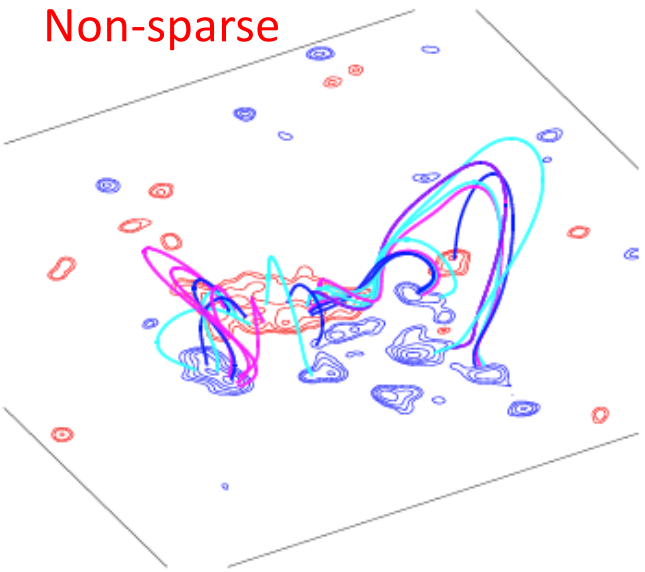

(a)

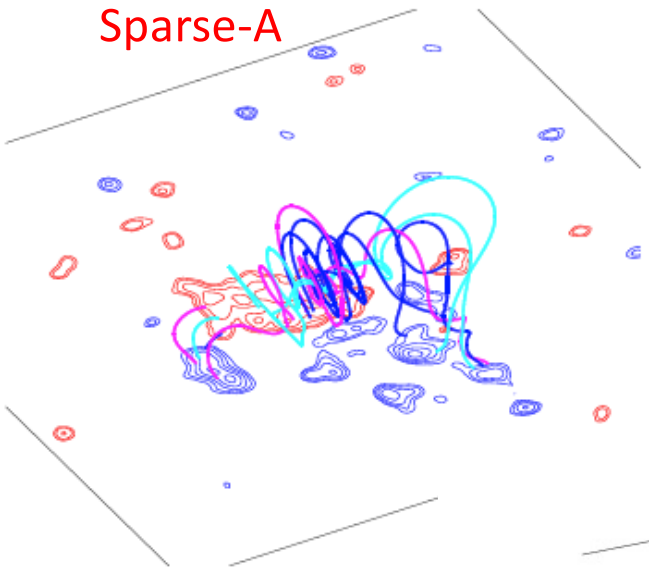

(b)

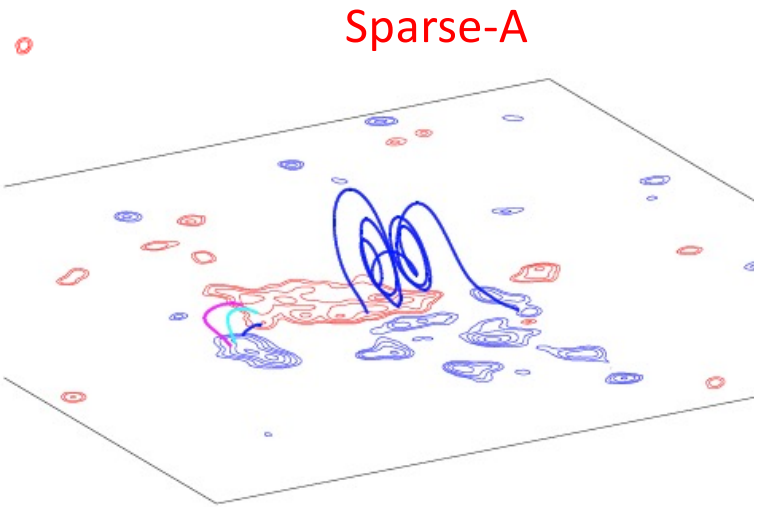

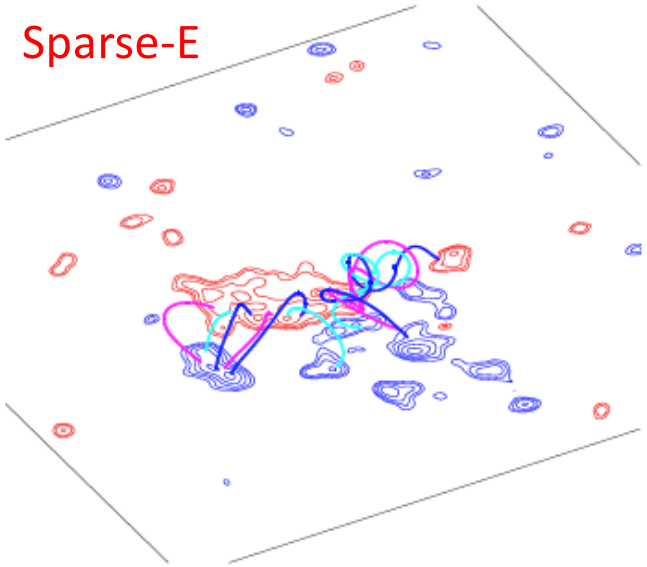

(c)

Origin of Highly Twisted Field lines

- 2nd December 20:51 UT

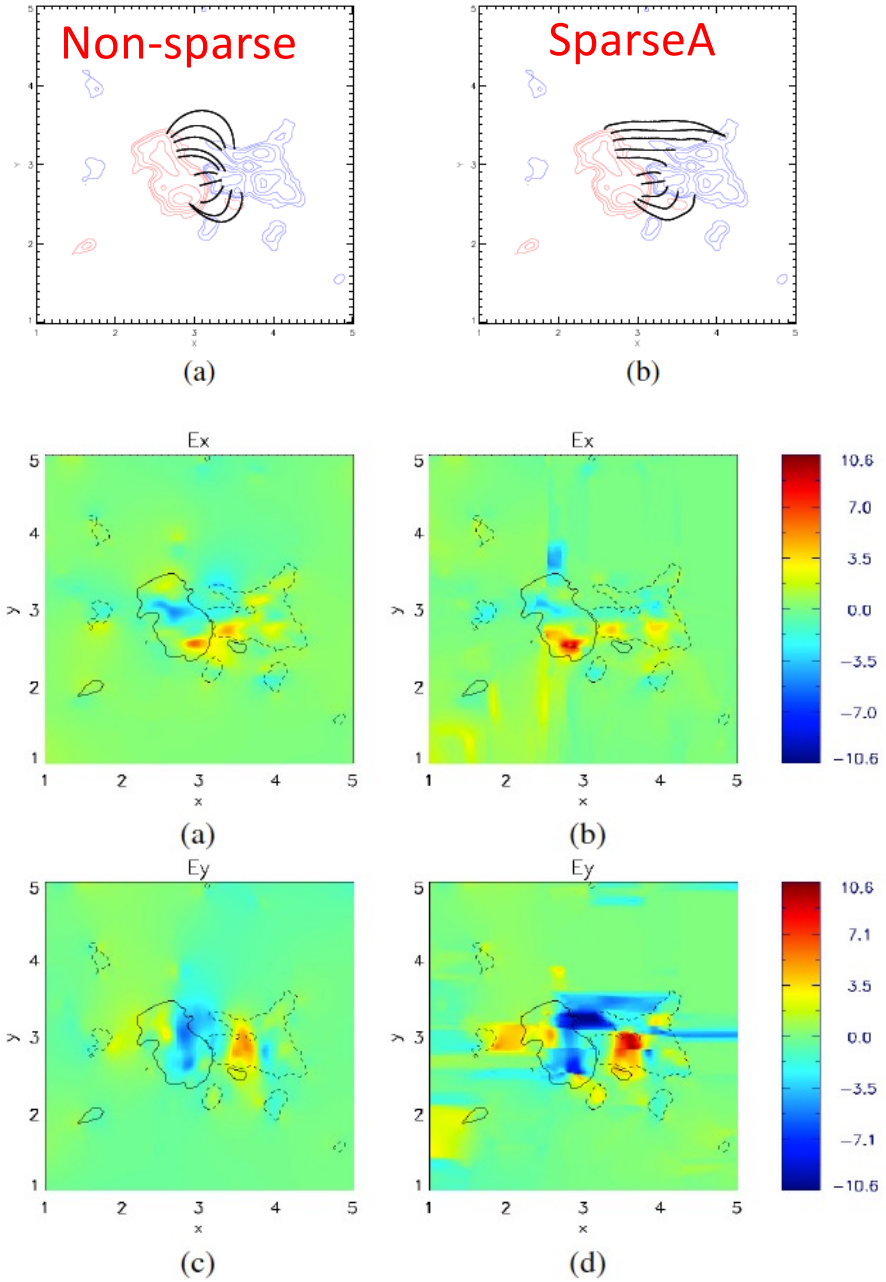

- 5nd December

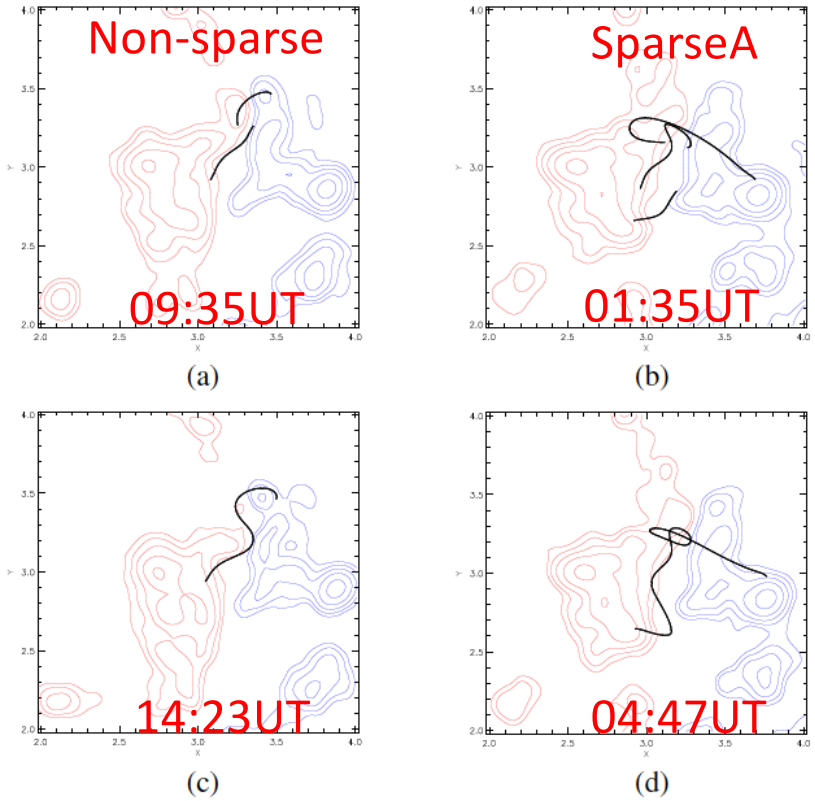

- Sparse approach has strong electric field between spatially separated polarities.
- Injection of strong horizontal field: leads to high energy, helicity and twist.

Varying Parameters

- Considered the effect of varying start time and non-ideal term

Non-ideal

Start time
4th Dec
06:24

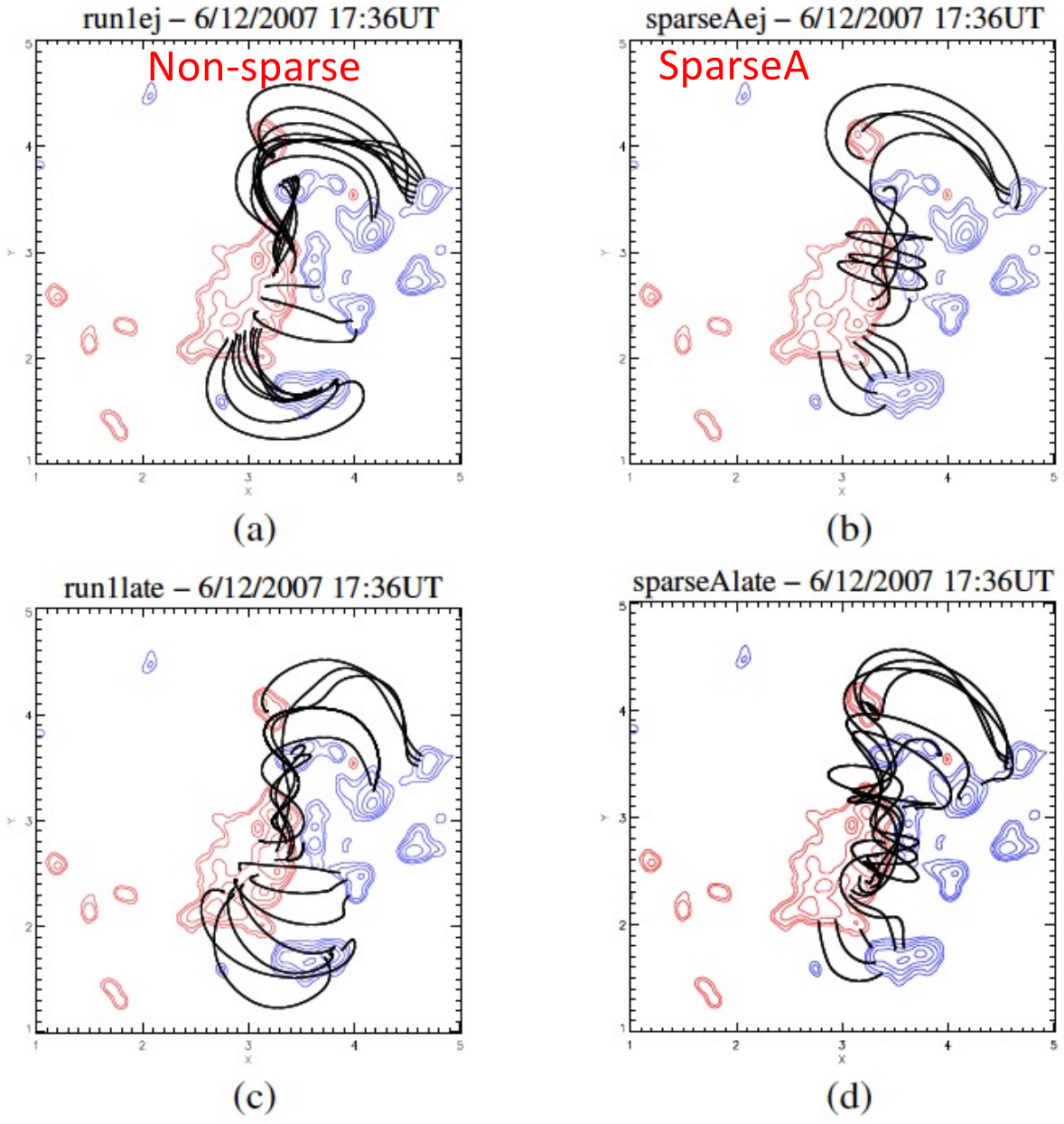

Summary

- Have compared Mackay et al. (2011) and Yeates (2017) electric field inversion techniques for normal component magnetograms.

- Mackay et al. (2011) – consistent solving for **E** and **A**
  produces a good match with observations (not perfect)
  positive helicity – forward-S sigmoid

- Yeates (2017) – inconsistent when solving for **E** and **A**
  E: negative helicity – inverse-S sigmoid.
  A: positive helicity – forward-S sigmoid.
  produces highly twisted fields – helical field line in vertical planes
  order of magnitude greater helicity.

- Yeates (2017): more consistent with Ohm's law.
  - strong electric field and injection of very strong axial field between spatially separated polarities

- Mackay et al. (2011) – break Ohm's law in many places
  - weak electric field that not significantly effect the corona.

- Which is best ?

Future Work

- Significantly behind schedule !

- Develop a new technique to evolve the field at two heights:
  - Bv at solar photosphere
  - Bv at chromosphere or low corona
  - Use **A** – magnetic vector potential - div **B** **= 0,** to machine precision.